19th Annual General Assembly – AGA 2018
International Association of Maritime Universities (IAMU)
R. Bosch-Tous, P. Casals-Torrens, J. Alvarez-Florez and A. Serrano-Fontova **(Eds)**

HYBRID GAS-ELECTRICAL POWER & HEAVY DUTY PROPULSION: TEST PLATFORM

R. Bosch[1, 2], P. Casals-Torrens[1, 2], J. Alvarez-Florez[3], Alexandre Serrano-Fontova[2,*]

[1]Barcelona School of Nautical Studies (FNB/UPC-BarcelonaTech)
[2]Department of Electrical Engineering
[3]Department of Thermal Machinery
Universitat Politècnica de Catalunya – BarcelonaTech
Pla de Plau, 18, 08003 Barcelona, Spain
e-mail: alexandre.serrano@upc.edu, web page: http://www.fnb.upc.edu

Keywords: Hybrid power systems, liquefied natural gas, heavy-duty propulsion systems, electrical systems, small vessels, technology impact, control and regulation, mariner engineers, training, education.

Abstract. This paper presents the results and discussion of an extensive set of tests of a hybrid generation system (gas-electric), to feed the electric electrical motors which propel a small or medium vessel. Primarily, the hybrid electric system includes a combustion engine, an electric generator and electric induction motors. The diesel engine represents the central part in regards to the propulsion task [1][2]. Thus, it provides the energy required by the electrical system, also supports load variations at low speed or cruising speed. Furthermore, it feeds other critical loads such as lights, electronic navigation systems, ancillary systems and other comfort loads within the hotel facilities. Presently, many technical challenges associated with the design of hybrid-electric propulsion systems are under discussion. Regarding technical limitations, the loading level and perhaps even more important is to deal with the complexity of the hybrid systems. Concerning to technical limitations, we can, therefore, highlight the following issues; the pilot excitation control, the performance of crash-stop manoeuvre and lastly the protection and control task.

1 INTRODUCTION

Albeit the most common type of propulsion in the maritime field are the engine-motors with an implemented propeller, however, in the recent years the interest to promote the electrical propulsion, have become a topic of undeniable scientific scrutiny. The aim of this interest is twofold; on the one hand, the reduction of the emission gases by using liquified natural gas (LNG) as a primary raw material [3]. Secondly, to test the behaviour of the electrical motors in regards of traction purposes. Accordingly, the required elements to accomplish this type of propulsion are as follows: a heat engine, a synchronous generator, the generator control systems and the electric motors. This paper shows the theoretical analysis of this electrical system its main features, the results of several tests carried out to validate the hypothesis. From the tests performed, it can be safely concluded that the system under investigation competes favourably and is capable of overcoming the severest system contingencies regarding the direct on-line start motors [4][5][6][7]. Lastly, it is crucial to note that the present study reveals the fact that, not only the ship is able to continue operating after a sever contingency but also the protection systems are properly designed so as to not misscoordinate in these scenarios.

2 TEST SYSTEM COMPONENTS DESCRIPTION

This section devotes to enumerate and make a thorough explanation of the elements that compose the system under investigation. The test platform was the whole system could be observed is depicted in Fig. 1. From Fig. 1, it is possible to observe the heat engine, the generator coupled with it, the induction machines and the system control that contain the circuit breakers (CB) and the adjustable-speed drive(ASD).

(a)

(b)

Figure 1: Test platform. Hybrid gas-electrical power & propulsion

2.1 Heat engine

The main element of the system is a heat engine, which acts as a prime mover. The data of the heat engine is detailed hereunder:

- Engine capacity: 8.8 litres
- Nº of cylinders: 8
- Power output: LNG at 1500 m^{-1}, 94 kW (50 Hz); 1800 m^{-1}, 113 kW (60 Hz)
- Power output: NG at 1500 m^{-1}, 82 kW (50 Hz); 1800 m^{-}1.99 kW (60 Hz)
- Engine in late [mm Hg] at 1500 m^{-1} 26 y 1800 m^{-1} 31.6
- The mass flow rate of LNG at 1500 m^{-1} 23 y 1800 m^{-1} 59

As can be seen, the power output, operating at the synchronous speed, that is to say, at 50 Hz and using LNG as a prime material, the output engine is 94 kW.

2.2 Electrical generator

This section aims at detailing the electrical generator, which uses the prime mover defined in the previous section to generate the required electrical power. The electrical generator is a brushless permanent magnet synchronous generator (PMSG). Specifically, the electrical generator incorporates a droop control system in regards the active-power/ frequency and reactive-power/voltage playing a pivotal role in transient studies during sever changes. Firstly, the frequency system control refers to the governor system, modifying the engine mass flow rate input to increase or decrease the torque applied to the shaft. Secondly, in the sense of voltage profile, the generator incorporates an automatic voltage regulator (AVR) to regulate the reactive-power injected. Purposefully, the electrical generator acts in fact, as a swing bus. The main features of the generator are detailed below:

- S = 175 kVA
- V = 400 V
- I_n = 252 A
- $I_{short\text{-}circuit}$ = 752 A
- Mass = 659 Kg
- Inertia = 1.93 kgm^2

where S is the rated apparent power, V is the rated output voltage, I_n represents the current voltage at rated power, $Is_{hort\text{-}circuit}$ is the current during a solid short-circuit at the main terminals. The electrical characteristics of the generator are detailed below:

- Permanent reactance, direct axis (X): 1.85 p.u
- Transient reactance, direct axis (X'd): 0.16 p.u
- Subtransient reactance, direct axis (X''d): 0.11 p.u

- Permanent reactance, quadrature axis(Xq): 1.12 p.u
- Subtransient reactance, quadrature axis (X''q): 0.15 p.u
- Leakage reactance (Positive sequence) (X_l): 0.07 p.u
- Negative sequence reactance (X_2): 0.11 p.u
- Zero sequence reactance (X_0): 0.07 p.u
- Transient time constant (T'd): 0.042 s
- Subtransient time constant (T''d): 0.012 s
- Transient time constant (T'd): 0.042 s
- Field time constant (T'_{do}): 1.1 s
- Armature time constant (Ta): 0.012 s
- Base rating for reactance values: 175 kVA
- Permanent short circuit current of the machine is 1.4 kA.

2.3 Induction machines

Since the induction motors (IMs) are the elements responsible of the propulsion coupled with the propellers, the parameters not only in steady state but also in the transient process are crucial. Purposefully, the data of the IMs is detailed further on:

1. IM A: 55 kW

S_n= 55 kW, V_n=0.38 V; I_n= 445 A; I_s= 720 A, I_0= 27 A; J: 0.8 kgm^2, f= 50 Hz, pf =0.85

2. IM B: 22 kW

S_n= 22 kW, V_n= 0.38 V; $\mathcal{p}$ = 1 I_n= 230 A; I_0= 10 A; I_s= 240 A f= 50 Hz, J: kgm^2, pf =0.85

where V_n is the rated voltage, I_n is the rated current, I_0 is the no-load current, I_s is the starting current, $\mathcal{p}$ represents the IM pole pairs, J the inertia of the IM, f is the rated frequency and lastly, pf is the rated power factor. The electrical parameters of the machine A and B are respectively;

1. IM A: r_s =0.038 Ω, r_r =0.045 Ω, l_r = 2.38e^{-2} H, l_s =2.38e^{-2} H, l_μ =2.2e^{-2} H

2. IM B: r_s =0.13 Ω, r_r =0.15 Ω, l_r = 4.9e^{-2} H, l_s = 4.9e^{-2} H, l_μ =4.85e^{-2} H

Finally, note, however, that the third motor (IM C), is equal to IM B.

2.4 Excitation system

As a brushless generator, the automatic voltage regulator (AVR) forms part of the excitation system, that is, the excitation power required by the PMSG. The AVR senses the altern current (AC) signals at the main generator winding and controls the excitation in order to maintain the generator output voltage within the specified limits. On the other hand, the maximum excitation is limited to a short period for safety, and in case it is exceeded, the AVR will be shut down. The AVR data is listed below:

- AC Power input from the PMSG (Max. values): V_n= 170-220 V, 3 phase, 3 wire, I_n= 3 A/phase and f = 100-120 Hz.

- DC Output of the AVR (Max. values): V_n= 120 V, I_n= 3.7 A (permanent) and I_{max}= 6 A (for 10 s)

On the second hand, the protections incorporated in the generator are listed below:

- Under frequency protection (UFP): The UFP is set to 95 % of the rated frequency, that is, 47,5 Hz, a slope of frequency of 100-300% below the 30 Hz, and also a maximum swell of 20% at the recovery is accounted.

- Overcurrent protection: The current limiter acts in case of a fault, and besides to limit the starting current of the generator. The protection considers a 10 s time delay.

- Over voltage protection (OVP): The OVP is set to 300 V with a fixed time delay of 1 s.

- Over excitation protection (OEP): This feature, allows the system to shut down the system in case of the DC field voltage of the excitation system exceeds 75 V considering a time delay of 8-15 s.

- Dip/Swell adjustment: These settings belong to a drop in voltage as well as an under-voltage (voltage dip) and an over-voltage (Swell), limiting the increasing volts per hertz (V/Hz). For our purposes, these settings are disabled.

- Droop control: The system, as a unique generator, it is acting as a swing bus considering droop adjustment to regulate 5% of voltage drop at full load zero power factor. Secondly, the stability adjustment is expected to control the relation V/Hz within the stable boundaries for a good transient and steady-state response. Additionally, the governor system acts by adjusting the mass flow rate of so as to increase the torque applied to the shaft and increase the active-power.

On the second hand, the protections incorporated in the generator are listed below:

1. Under frequency protection (UFP): The UFP is set to 95 % of the rated frequency, that is, 47,5 Hz, a slope of frequency of 100-300% below the 30 Hz, and also a maximum swell of 20% at the recovery is accounted.

2. Overcurrent protection: The current limiter acts in case of a fault, and besides to limit the starting current of the generator. The protection considers a 10 s time delay.

3. Overvoltage protection (OVP): The OVP is set to 300 V with a fixed time delay of 1 s.

4. Overexcitation protection (OEP): This feature, allows the system to shut down the system in case of the DC field voltage of the excitation system exceeds 75 V considering a time delay of 8-15 s.

5. Dip/Swell adjustment: These settings belong to a drop in voltage as well as an under-voltage (voltage dip) and an over-voltage (Swell), limiting the increasing volts per hertz (V/Hz). For our purposes, these settings are disabled.

6. Droop control: The system, as a unique generator, it is acting as a swing bus considering droop adjustment to regulate 5% of voltage drop at full load zero power factor. Secondly, the stability adjustment is expected to control the relation V/Hz within the stable boundaries for a good transient and steady-state response. Additionally, the governor system acts by adjusting the mass flow rate of to increase the torque applied to the shaft and increase the active-power.

3 THEORETICAL ANALYSIS

The present section seeks to address the transient stability during the transient behavior of the IMs during its starting and also the transient system response under severe changes in load torque during operation. Since the PMSG is the unique generator, the classical theory of stability applied to our isolated system. Regarding system

stability, this section recalls the theory basics briefly in the case of study. As a matter of fact, the magnitudes involved are normally analysed separately in powers system stability and is as follows: voltage angle stability, voltage stability and frequency stability [8], which in turn, these are highly linked between each other, especially here. It is nonetheless important to note that, depending on the severity of the disturbance, the stability can be a large disturbance and small disturbance. Herein, the system stability is discussed for the particular system defined in the previous section and is detailed hereunder.

The set of equations which govern the transient behaviour are considered by the set of differential-algebraic equations (1):

$$\begin{aligned} \frac{d\omega_i}{dt} &= \frac{\omega_o}{2H}[Pm_i - Pe_i(\delta_i) - \frac{D_i}{\omega_o}(\omega_i - \omega_o)] \\ \frac{d\delta_i}{dt} &= \omega_i - \omega_o \end{aligned} \tag{1}$$

$$\Delta\delta = \int \Delta\omega \; dt = 2\pi \int \Delta\delta \; dt \tag{2}$$

$$\begin{aligned} Pe_i &= \Re\{E_i \cdot I_{i,g}{}^*\} = \frac{E_i \cdot U_g}{jX'} \sin\delta_i \\ I_{i,g}{}^* &= \frac{E_i - Ug_i}{jX'_i} \end{aligned} \tag{3}$$

Where P_g is the mechanical power of the generator in node *i*, P_{ei} is the electrical power delivered by the generator *i*, respectively. P_{ei} can be computed as in (3) D_i is the damping factor of generator i, ω_i is the electrical speed of every i generator, ω_0 is the synchronous electrical speed and H_i inertial constant for each one, E_i is the generator voltages and δ_i is the generator phase angle behind the synchronous reactance ($Ei\angle\delta i$), Ug_i is the voltages of the generators after the transient reactance, I^* is the conjugated current, jX'_i the transient reactance of each generator and *i= 1*. E_i is the generator voltages of each one, B_{ij} is the line susceptance and G_{ij} the line conductance, both can also be expanded into generator buses. The compact expression of (1), is given in (3).

$$\begin{aligned} \dot{x} &= F(x,u) \\ 0 &= g(x,u) = YU - \mathrm{I}_i(x,u) \end{aligned} \tag{3}$$

where x is the state vector, $\dot{x}$ is its derivative, F is sufficiently differentiable, Y is the admittance matrix of the system considering the loads and lines, U is the bus voltages of this buses and I_g the current injected by the unique generator, which at same time depend on the state variables and also on the voltage buses. In our particular system, the state vector is composed by the transposed vector defined in (4):

$$x^T = [\delta_g, \omega_g] \tag{4}$$

In this stage, it is crucial to point out that, if the rotor of the machine the angular speed increases, therefore, the angle gets unstable and the frequency of the system will also be increased, whilst in case that the speed decreases, the angle will also be unstable and, the system will reach an under frequency operation. In this sense, it is essential to consider the generator inertia, which acts by damping the system. Notwithstanding the preceding, the frequency oscillation, as is observable from (2) is related to the rotor speed, wherewith the frequency drop will be evaluated to observe the system response against the severe requirement in IM starting.

Since the severest transient accounted here is an IM starting, where the required power is mainly reactive, the voltage dip duration and deep depend essentially on the required time to reach the stable operation and secondly on the relation between the short-circuit ratio (S_{sc}) in p.u. where the IM is connected and the starting current. As a

consequence, the short circuit ratio and is considered in (5) and the root-mean-square (RMS) permanent three-phase short circuit at the PCC is calculated in (6):

$$S_{sc} = \frac{1}{jX_d} \tag{5}$$

$$I_{sc} = \frac{S_{sc}}{\sqrt{3} \cdot U_n} \tag{6}$$

where the jX_d is the direct-axis reactance of the machine in p.u. Since the reactance of the IM during the starting process is variable and depends directly on its slip, the expected RMS voltage value during this transient process, depends on the relation between the short-circuit power value at the PCC, which belongs in this case to the short-circuit power at the generator terminals and the IM starting current.

The stability is controlled by the AVR which has the capability to increase or decrease the third term of the equation defined in (1). Consequently, this term can be otherwise expressed as (7):

$$\frac{D_i}{\omega_o}(\omega_i - \omega_o) = k_2 \Delta E_q' \tag{7}$$

Considering that the term $\Delta E_q'$ makes changes in the machine flux, by increasing or decreasing field voltage and k_2 is a constant, it is worth noting that this term can enhance the system stability, by damping the oscillations. Thus, the AVR acts increasing the system stability and is of utmost importance to consider its time response.

4 TEST MEASUREMENTS

4.1 Test 1

This test considers the direct on-line starting of the IM A to observe the response of the generator in these conditions and also to detect if the system is close to a voltage or frequency collapse.

Here, in Fig.2 it is easy to observe the fact that a voltage dip occurred during the motor starting, the values during this process are summarised below:

- I_s=480 A; I_s(t=1s)=130 A , I_o= 27 A
- V_{RMS}= 150 V

The IM takes 540 ms to reach its rated speed, due to the starting current the voltage dip is observed, however, the voltage recovery takes place after 620 ms. In this sense, the voltage regulator senses the over-voltage and injects the required reactive power to recover the situation. Unfortunately, the accuracy of the AVR regarding its time-response reaches an over-voltage following the IM recovery. The AV produces this slight oscillation. In addition to the above mentioned earlier, and expected from the theoretical analysis, the frequency oscillation of 18 Hz takes place the first ms and afterwards and thanks to the AVR operation, the system recovers.
The active and reactive powers are depicted in blue and pink respectively, the voltage and current waveforms and its respective RMS values (V_1 red, V_2 green, V_3 blue) and lastly the frequency value is plotted in black.

4.2 Test 2

This test considers the direct on-line starting of the IM B in order to observe the response of the generator in these conditions and also to detect if the system is close to a voltage or frequency collapse.

Here, in Fig. 3 it is easy to observe the fact that a voltage dip occurred during the motor starting, the values during this process are summarised below:

- I_s=180 A; I_s(t=1s)=100 A , I_o= 10 A
- V_{RMS}= 300 V

The IM takes 164 ms to reach its rated speed, due to the starting current the voltage dip is observed. However, the

voltage recovery oscillation lasts 1.5 s due to the time-response of the AVR system. In this sense, the voltage regulator senses the over-voltage and injects the required reactive power to recover the situation. In this stage, the over-voltage post-recovery is weaker because the lower is PCC voltage droop, the higher is the AVR voltage excitation increasing. As commented in the previous test, and also expected from the theoretical analysis, the frequency oscillation of 8 Hz takes place the first ms and afterwards and thanks to the AVR operation, the system recovers.

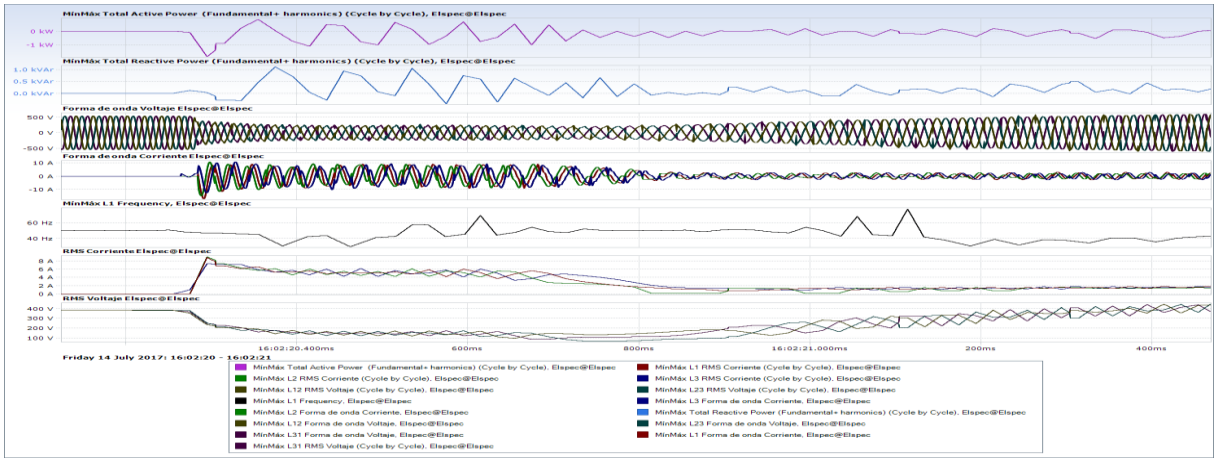

Figure 2: Electrical parameters of TEST 1

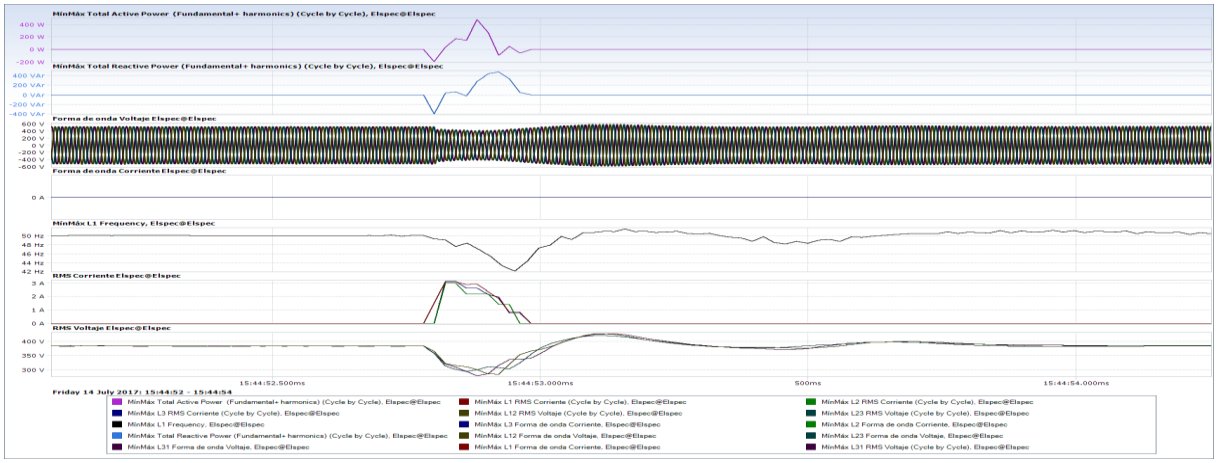

Figure 3: Electrical parameters of TEST 2

The active and reactive powers are depicted in blue and pink respectively, the voltage and current waveforms and its respective RMS values (V_1 red, V_2 green, V_3 blue) and lastly the frequency value is plotted in black

4.3 Test 3

This test considers the direct on-line starting of the three IMs in the following order; firstly, the IM B, afterwards the IM A and lastly the IMC. In these conditions, it is possible to observe the effects of a full test as well as to detect if the system is close to a voltage or frequency collapse not only during starting but also during steady-state operation. Here, in Fig.1 it is easy to observe the fact that a voltage dip occurred during the motor starting, the values during this process are summarised below:

- I_s=180 A, I_o= 10A (Motor B)
- I_s=480 A, I_o= 28 A (Motor B+A)

- I_s=172 A, I_o= 55A (Motor B+A+C)
- I_o= 41 A (Motor A+B)
- I_o= 28 A (Motor A)

The results from the previous subsections 4.1 and 4.2 are equally observable here, note, however, that the no-load current is now an important factor. As can be seen in Fig. 4 the frequency and voltage drop during starting IM B and C are similar, but the drop in IM C is lower, and this is because IM A and B are acting transiently as generators during its starting. The active and reactive powers are depicted in blue and pink respectively, the voltage and current waveforms and its respective RMS values (V_1 red, V_2 green, V_3 blue) and lastly the frequency value is plotted in black.

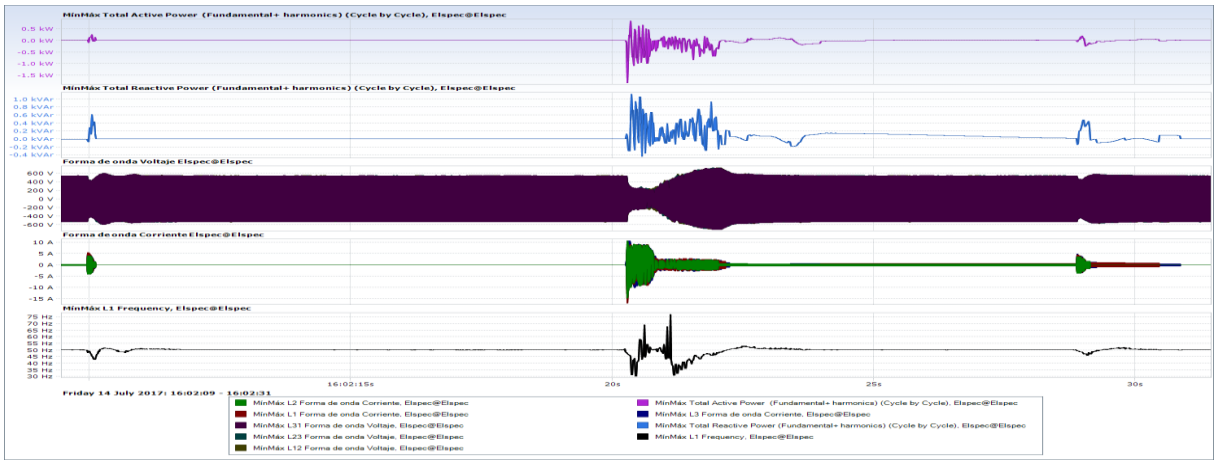

Figure 4: Electrical parameters of TEST 3

6 CONCLUSIONS

At first sight and observing the tests carried out it seems altogether reasonable and logical to assert that the system will remain stable following the severe transients, regarding voltage and frequency.

Firstly, it can be seen that for the most severe transient, as expected, occurs during IM A starting and the temporary system loss of frequency and voltage is relevant, however, after 540 ms the system recovers. We can safely conclude that, in these conditions and considering a temporary droop, the frequency and voltage oscillations are within acceptable boundaries and do not produce protective nuisance tripping.

Secondly, the performance of the AVR competes favourably and assures that the system will remain stable following all possible disturbances. As a matter of fact, during a 0.6 deep voltage droop, the under-voltage does not trips, which is crucial in maritime operations.

Thirdly, it is also a transcendental factor to consider the system inertia, considering that the heat-engine output is 90 kW and the electrical generator is 175 kVA, this fact reveals that the rotating masses reduces the frequency droop and also enhances the system stability. Therefore, oversizing the electrical generator, we achieve a less reduction in voltage and frequency in the heaviest requirements because the total inertia of the shaft (engine plus generator) is acting as a “kinetic energy recovery system”.

Fourthly, it has been demonstrated that the propeller power is proportional to the absorbed current, which will result in a valuable mnemonic tool to maritime personnel. In this sense, this tested platform seems to be suitable not only for academic purposes but also for the private maritime company formation personnel.

Additionally, the system accounted here will help in reducing the CO_2 emissions, which is one of the main short-term concerns in maritime transportation and besides, it has been proved that an LNG-based engine with a set of IM is capable of propelling the system and notably enhances the time response of the ship. Especially, in the most challenging operations such as the “crash stop,” when this is particularly crucial in preventing hazardous events.

Lastly, the immersed IM within an IP 58 protection, allows its vertical subjection, and as a consequence, the group improves its propeller mobility, which, in turn, helps the system in addressing extreme situations.

ACKNOWLEDGEMENTS

The authors would like to wholeheartedly thank the financial support and the great willingness to collaborate towards this project of GECRIO, SEALINK and GAS NATURAL FENOSA. Undoubtedly, without these private efforts, the project would have been impossible to carry out.

REFERENCES

[1] J. L. Kirtley, A. Banerjee, and S. Englebretson, "Motors for Ship Propulsion," *Proc. IEEE*, vol. 103, no. 12, pp. 2320–2332, 2015.

[2] Z. Liu, J. Wu, and L. Hao, "Coordinated and fault-tolerant control of tandem 15-phase induction motors in ship propulsion system," *IET Electr. Power Appl.*, vol. 12, no. 1, pp. 91–97, 2018.

[3] G. Sulligoi, A. Vicenzutti, and R. Menis, "All-Electric Ship Design: From Electrical Propulsion to Integrated Electrical and Electronic Power Systems," *IEEE Trans. Transp. Electrif.*, vol. 2, no. 4, pp. 507–521, 2016.

[4] S. Tanneeru, J. Mitra, Y. J. Patil, and S. J. Ranade, "Effect of Large Induction Motors on the Transient Stability of Power Systems," vol. 88003, pp. 223–228, 2007.

[5] J. C. Das, "Effects of Momentary Voltage Dips on the Operation of Induction and Synchronous Motors," *IEEE Trans. Ind. Appl.*, vol. 26, no. 4, pp. 711–718, 1990.

[6] D. S. Brereton, D. G. Lewis, and C. C. Young, "Representation of Induction-Motor Loads During Power-System Stability Studies," *Trans. Am. Inst. Electr. Eng. Part III Power Appar. Syst.*, vol. 76, no. 3, pp. 451–460, 1957.

[7] A. H. Kasem Alaboudy, H. H. Zeineldin, and J. Kirtley, "Microgrid stability characterization subsequent to fault-triggered islanding incidents," *IEEE Trans. Power Deliv.*, vol. 27, no. 2, pp. 658–669, 2012.

[8] P. Kundur *et al.*, "Definition and Classification of Power System Stability IEEE/CIGRE Joint Task Force on Stability Terms and Definitions," *IEEE Trans. Power Syst.*, vol. 19, no. 3, pp. 1387–1401, 2004.